Formation and Corrosion Resistance of Amorphous Ti Base Alloys

M. Naka[a], T. Okada[b] and T. Matsui[b]
[a]Welding Research Institute, Osaka University, Mihogaoka 11-1, Ibaraki, Osaka 567, Japan
[b]Graduate Student, Osaka University

Corrosion resistant amorphous Ti-B and Ti-Si alloys were prepared on various substrates by RF sputtering. The alloying of B content of 8 at% or more stabilizes the amorphous structure. The corrosion properties of Ti alloys were evaluated by measuring the polarization curves in 1N HCl. Although the addition of B to crystalline bulky Ti shifts the corrosion potentials of Ti to the less nobles of -0.5 V(SCE) or less, that of B to amorphous sputtered Ti moves the corrosion potentials to the noble side of +0.3 V(SCE). The current densities of amorphous Ti-B alloys at 0.1V(SCE) of the passive state are lower than that of the crystalline bulky alloys. Ti-Si sputtered alloys were amorphous at the silicon content of 12 at% or more. The amorphous Ti-Si alloys also show superior corrosion resistance, compared the crystalline Ti-Si alloys.

1. Introduction

The application of materials in new engineering fields needs more corrosion resistant alloys. The new corrosion resistant alloys has been developed by two methods, which are the alloying of large amounts of corrosion resistant elements such as chromium, and the purifying of corrosion resistant alloys. We have now the third method to improve the corrosion resistance of alloys. Amorphization from crystalline structure of alloys gives alloys high corrosion resistance since amorphous alloys have no defects of precipitates and crystalline boundaries which are initiates of corrosion[1].

Naka et al.[2-4] reported that amorphous stainless iron, cobalt and nickel alloys showed high corrosion resistance. Titanium is also another candidate materials for corrosion resistant alloys. Amorphous titanium alloys containing P as a glass forming element which were produced from liquid state exhibited high corrosion resistance[5].

The amorphous alloys were so far prepared by rapid quenching molten alloys on highly rotating copper wheel to obtain high cooling rates. The high cooling rates prevents to nucleate crystals from liquids. Vapor quenching also provides easy process to make amorphous alloys and coats them on various substrates[6].

. This paper tries to improve corrosion resistance of titanium by amorphizing using alloying elements of B and Si as glass forming elements in sputtering process, and clarifies corrosion properties of amorphous Ti-B and Ti-Si alloys .

2. Experimental procedure

RF magnetron sputtering technique was used to prepare amorphous alloys in low pressure argon gas of 6.65 MPa. Targets used were 100 mm in diameter and 5 mm thick and were composed of Ti and B or Ti and Si. The substrates of aluminum were water cooled.
The main sputtering conditions were water cooled. The main sputtering conditions were a sputtering power and time of 600 W and 14.4 ks, respectively. The film thickness of the alloys prepared was 20 μm. The structure of sputtered films was investigated by x-ray diffractometry.

The corrosion behavior of the films was evaluated by measuring polarization curves in 1N HCl with a potential sweep rate of 2.5×10^{-3} Vs^{-1} in 1N HCl.

3. Results and discussion

Figs. 1 and 2 show the x-ray diffraction patterns of sputtered Ti-B alloys. The structures of alloys of No. 1 (0at%B) and No. 2(2.9 at%B) are hcp crystalline phase. The Ti-B alloys containing B content from 8 at% to 51 at% B which show only a few diffuse diffraction peaks are amorphous.

. By adding B content of 51 at% or more the Ti-B alloys become crystalline phases composed of Ti_3B_4 and TiB_2. The glass forming range of Ti-B is presented in Ti-B phase diagram. The addition of B to Ti makes Ti-B alloys in wide range of B content amorphous. It is known that alloys showing deep suppression of liquids temperature in eutectic reaction become easily amorphous. The melting points of Ti-B alloys definitely are suppressed by mixing B. This may imply that the amorphous structures of Ti-B alloys are also stabilized by mixing B to Ti. The amorphous Ti base alloys containing P were prepared by liquid quenching technique. Although the liquid quenching process restricts the composition range of amorphous alloys and the size of the alloys in ribbon type tape, the vapor quenching process provides the wide composition range of amorphous alloys and also the coated films on various substrates. The corrosion behavior of sputtered Ti-B alloys were investigated by measuring polarization curves of the alloys in aerated 1N HCl. Fig. 3 shows the polarization curves of sputtered crystalline Ti-B alloys containing B content of 0 to 2.91at% in 1N HCl. Though the crystalline pure Ti is passivated at potentials between 0 and +0.5 V(SCE), it actively dissolves at potentials of +0.5 V(SCE) or more. The sputtered Ti-B alloys with 2.91at% B and 5.18at%B are also passivated, but they shows less noble corrosion potential than 0 V(SCE). The polarization curves of amorphous Ti-B alloys containing B content of 12.67 at% B to 16.20 at% B are shown in Fig. 3. The corrosion potentials of Ti-B alloys are shifted from -0.3 V(SCE) of 5.18 at%B to +0.4 V(SCE) with increasing B content. The amount of boron hydroxide on the alloy surface at the natural
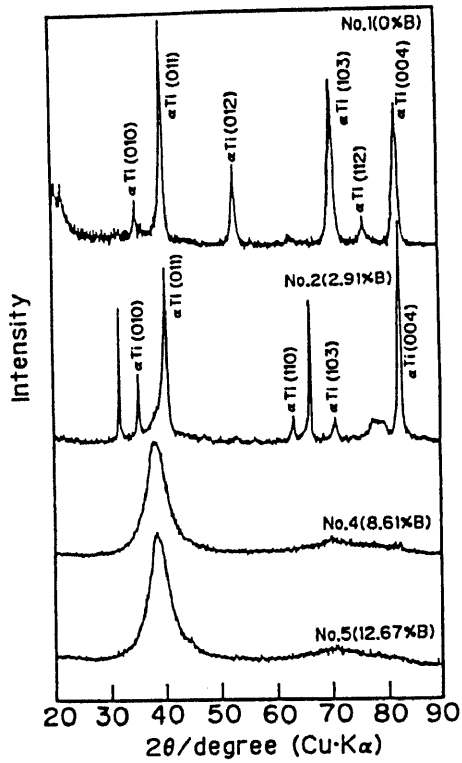
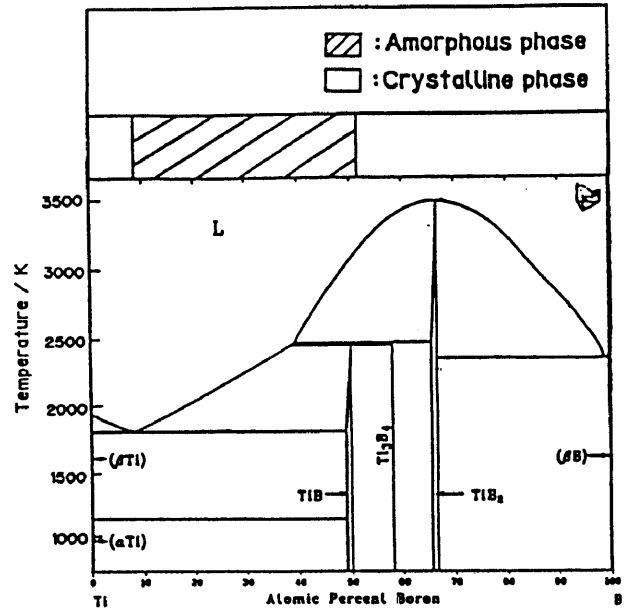Fig. 1 X-ray diffraction patterns of sputtered Ti-B alloys.
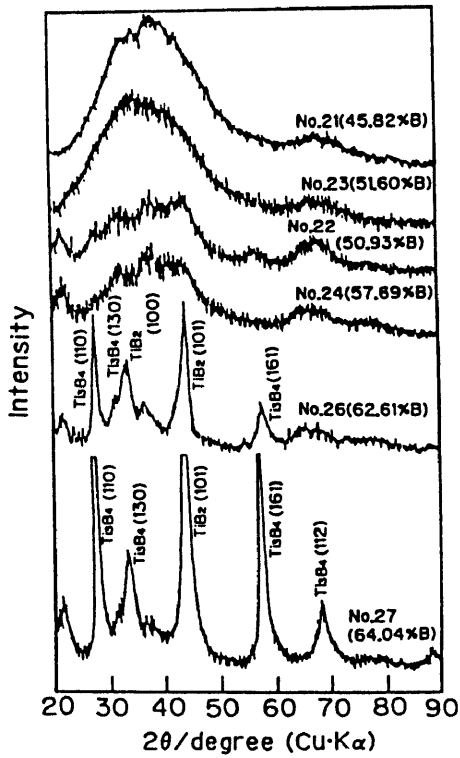
Fig. 3 Glass forming range of Ti-B alloys.

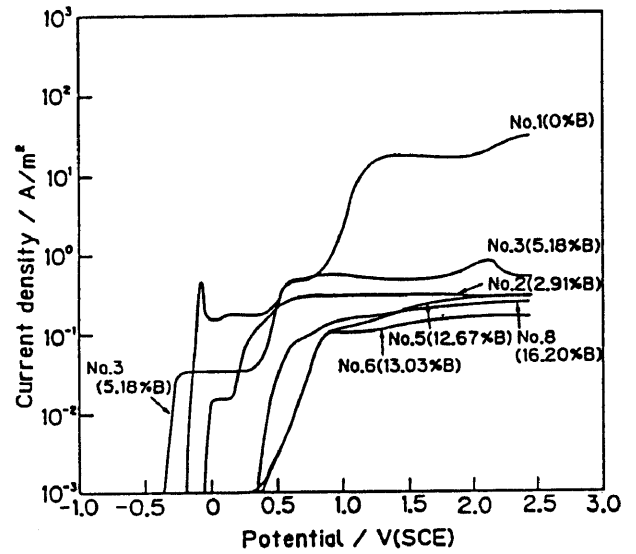Fig. 2 X-ray diffraction pattern of sputtered Ti-B alloys.

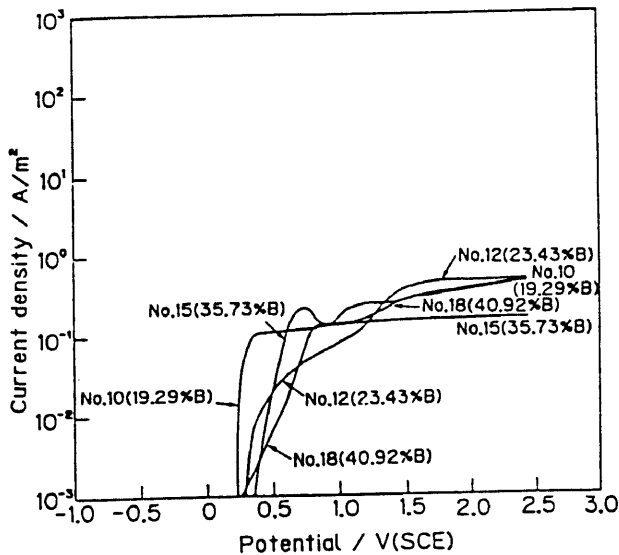Fig. 4 Polarization curves of sputtered crystalline and amorphous Ti-B alloys in 1N HCl.

Fig. 5 Polarization curves of Ti-B amorphous alloys in 1N HCl.

Fig. 6 Anodic polarization curves of Ti-B amorphous alloys in 1N HCl.

immersion state in 1N HCl may increase with increasing B content in Ti-B amorphous alloys. Amorphous Ti-B amorphous alloys are spontaneously passivated in 1N HCl. The current densities at the passive state of +0.5 V(SCE) or more for Ti-B amorphous alloys are definitely lower than that of sputtered pure Ti. This means that the amorphization of Ti-B alloys extremely improves the corrosion resistance of Ti, particularly in more positive potentials.

Fig. 5 represents the polarization curves of Ti-B amorphous alloys containing B content of 19.29 at%B to 40.92 at%B. The all amorphous alloys are spontaneously passivated after immersing in 1N HCl. The corrosion potential of the Ti-B amorphous alloys are around +0.3 V(SCE).

The current densities at the passive state for the Ti-B amorphous alloys are same value of about 10^{-1} A/m^2. After passivation the surface properties are the same in Ti-B amorphous alloys. Compared with crystalline pure Ti, the surface of the Ti-B amorphous alloys are very homogeneous and corrosion resistant. The amorphous Ti-B alloys have no defects such as precipitates and crystalline boundaries which operates as corrosion initiation sites.

Fig. 6 shows the polarization curves of amorphous Ti-B alloys with 45.8 at%B and 51.6 at%B and crystalline Ti-B alloys with 50.9 at%B and 64.0 at%B in 1N HCl. The amorphous Ti-B alloys containing high B content which are spontaneously passivated show lower current dsensities at the passive state. On the other hand, the crystalline Ti-B alloys containing high B content which are not passivated, and actively dissolve with increasing potential.
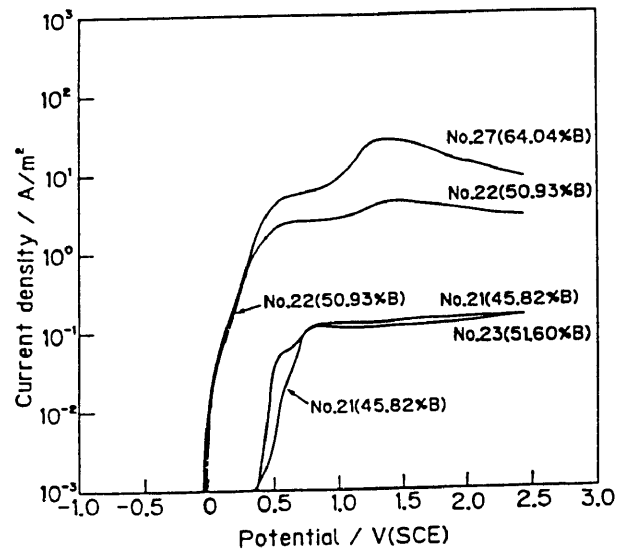
The sputter Ti-B alloys become crystalline by large amounts of boron of 51 at% or more, since the alloys have crystalline borides of Ti$_3$B$_4$ and TiB$_2$. The crystalline defects such as crystalline boundaries in the borides work as corrosion sites.

In order to make clear the role of amorphization of Ti-B alloys in corrosion behavior, the corrosion potentials of Ti-B sputtered alloys are plotted against B content in the alloys as shown in Fig. 7. The corrosion potentials of sputtered crystalline Ti-B alloys with small amounts of B content including pure Ti are around -0.3 V(SCE), and the potentials of crystalline Ti-B alloys with large amounts of B content are around 0 V(SCE). On the other hand, the Ti-B amorphous alloys containing B content from 12.67 at%B to 51.6 at%B shows higher corrosion potentials of +0.3-+0.4 V(SCE). The amorphization of structure makes to shift corrosion potentials of Ti-B alloys from 0 V(SCE) to nobler side of +0.3 V(SCE) or more. The corrosion potentials of the bulky crystalline Ti-B alloys including pure crystalline Ti are also included in Fig. 7. The corrosion potential of pure Ti does not change by sputtering, but the corrosion potentials of bulky crystalline Ti-B alloys are more less noble, compared with sputtered crystalline Ti-B alloys.

The crystalline bulky Ti-B alloys including TiB$_2$ are corrosive in 1N HCl, since the corosion potentials of the alloys are around -0.5 V(SCE). The passive current densities of sputtered Ti-B alloys at +0.1 V(SCE) are plotted in Fig. 8. The values of crystalline Ti-B bulky alloys are included in the figure. The passive current density of sputtered pure Ti is higher than that of crystalline Ti. This comes from that the micro crystalline film has the micro- defects as
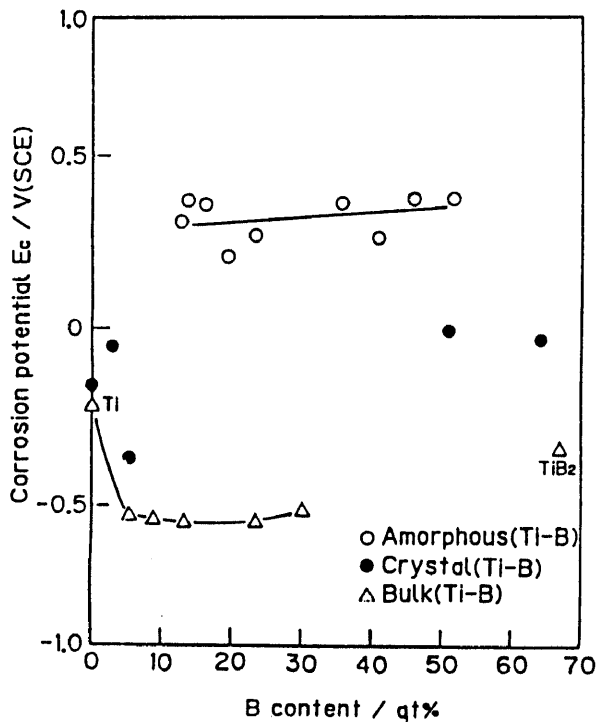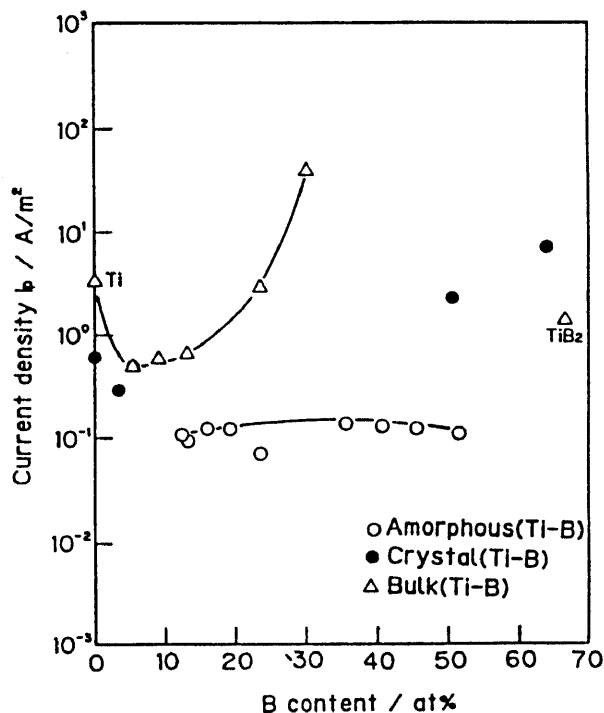
corrosion initiates. The passive current densities of sputtered crystalline Ti-B alloys show the minimum around B content of 10 at%B, and increase sharply with increasing B content. On the other hand, the passive current densities of amorphous Ti-B with B content from 15 at%B to 51 at%B is about 10^{-1} A/m^2, and one or two order of magnitude lower than that of the crystalline Ti-B alloys. Though the current densities of crystalline Ti-B bulky alloys are lower than that of crystalline Ti-B sputtered alloys, the values of the bulky alloys are larger than that of the amorphous alloys.

The amorphous Ti-B alloys is chemically homogeneous, and have no crystalline defects such as crystalline defects such as precipitates and grain boundaries which will operate as corrosion initiates in corrosive solutions. This is attributable to that the amorphous Ti-B alloys show more noble corrosion potentials and lower passive current densities than that of crystalline sputtered or bulky Ti-B alloys.

Figs. 9 and 10 shows the x-ray diffraction patterns of Ti-Si sputtered alloys containing Si content from 0 at%Si to 12 at%Si, and from 14 at%Si to 100 at%Si, respectively. The sharp x-ray diffraction peaks of crystalline hcp phase are indicated in pure Ti, Ti-6.4 at%Si and 12.0 at% Si alloys. Since Ti-11.5 at%Si and Ti-Si alloys containing Si content of 30 at% or more demonstrate the diffuse x-ray diffraction patterns of amorphous phases, the sputtered Ti-Si alloys containing Si content of 12 at%B or more are amorphous. Ti-Si alloys containing Si content around 80 at%Si indicate two first x-ray peaks at 30 degree and 40 degree, and are composed of two amorphous phases of Ti rich phase and Si rich phase.

The glass formation range of Ti-Si alloys is expressed in the Ti-Si phase diagram in Fig. 11. Compared with the glass formation range of Ti-Si alloys quenched from liquids[7], that of sputtered alloys are wider, composing of Si content from 12 at%Si to 100 at%Si. The corrosion behavior of sputtered Ti-Si alloys are investigated by measuring the polarization curves of the alloys in 1N HCl. Figs. 12 to 14 indicate anodic polarization curves of Ti-Si sputtered alloys in 1N HCl. As discussed in the behavior of sputtered Ti-B alloys, the sputtered pure titanium is passivated at potentials up to +0.5 V(SCE). The sputtered crystalline and amorphous Ti-Si alloys are spontaneously passivated in 1N HCl, and the passive state of the alloys are stable even at a high potential of +2.5 V(SCE). Compared with sputtered crystalline Ti-B alloys, the sputtered crystalline Ti-6.4 at%Si alloy is stable in 1N HCl. As the microstructures of both crystalline sputtered alloys are same, the difference of corrosion behavior of the alloys arise from the chemical properties of corrosion products composed of boron or silicon as a glass forming element in titanium. The corrosion product formed on the crystalline sputtered alloys may be more stable in Ti-Si alloy, compared with Ti-B alloy.

The Ti-Si amorphous alloys are high corrosion resistant, because the corrosion potentials of the alloys are in high noble side around +0.8 V(SCE), and the passive current densities are in the order of 10^{-1} A/m^2 or below. These results come from that the passive films on Ti-Si amorphous alloys after immersion in 1N HCl are very stable and high corrosion resistant. The high corrosion resistance of the Ti-Si alloys are also shown in Figs. 15 and 16, where the corrosion potentials and the passive current densities of sputtered Ti-Si alloys at +1.0 V(SCE) in 1N HCl are plotted against Si content.

Fig. 7 Compositional dependence of corrosion potential for Ti-B amorphous alloys, T-B crystalline alloys and Ti-B bulky alloys.

Fig. 8 Compositional dependence of passive current densities for Ti-B amorphous alloys, Ti-B crystalline alloys and Ti-B bulky alloys.
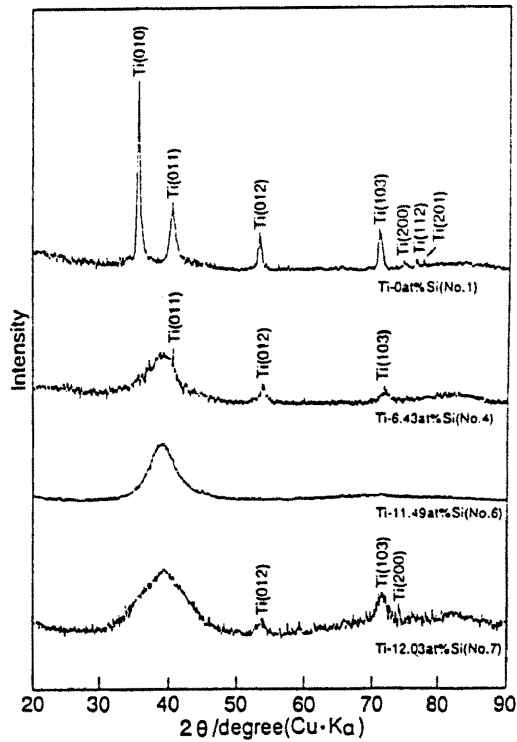
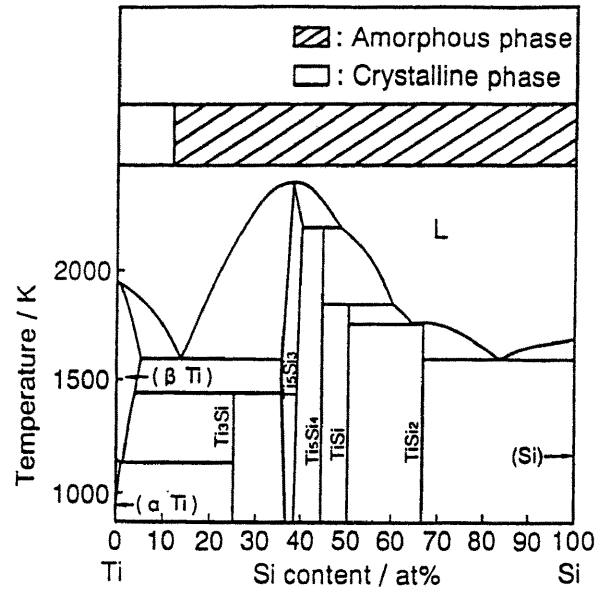Fig. 9 X-ray diffraction patterns of sputtered Ti-Si alloys.

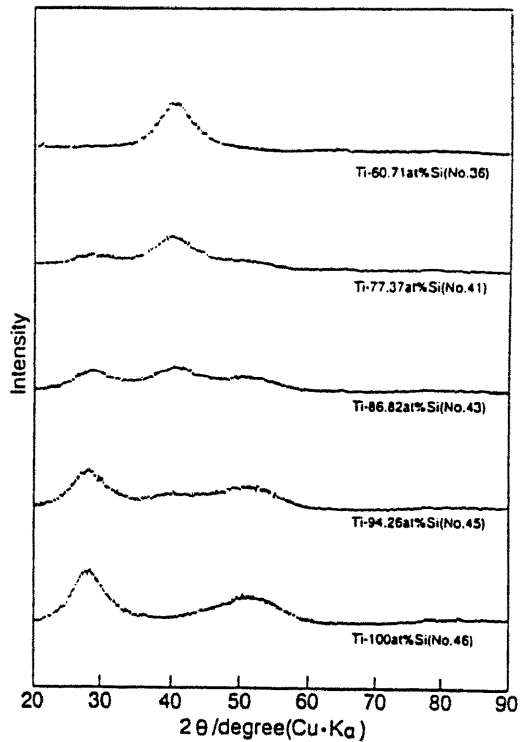Fig. 11 Glass forming range of Ti-Si alloys.

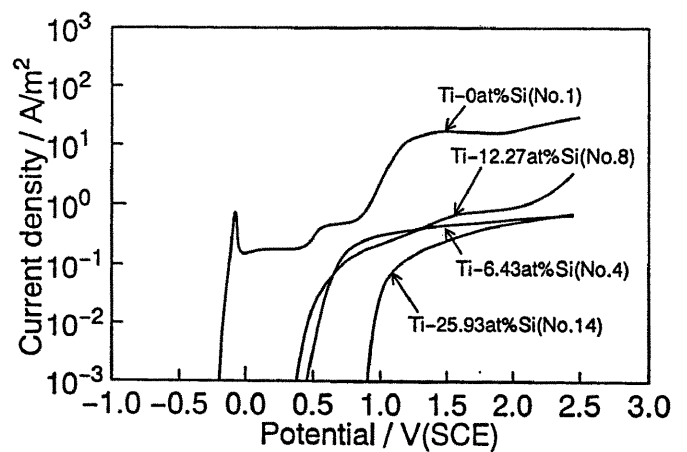Fig. 10 X-ray diffraction pattern of Ti-Si alloys.

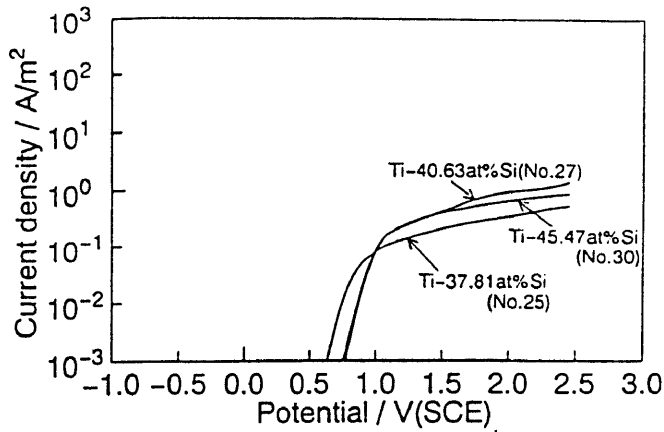Fig. 12 Anodic polarization curves of sputtered Ti-Si alloys.

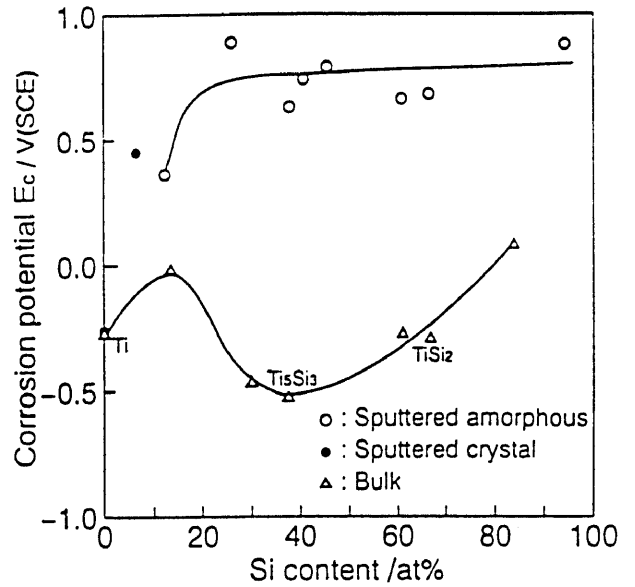Fig. 13 Anodic polarization curves of sputtered Ti-Si alloys.

Fig. 15 Compositional dependence of corrosion potential for sputtered amorphous , sputtered crystalline and crystalline bulky Ti-Si alloys.
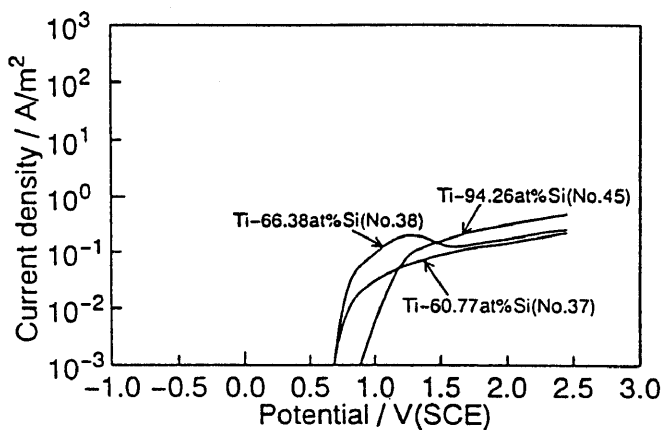

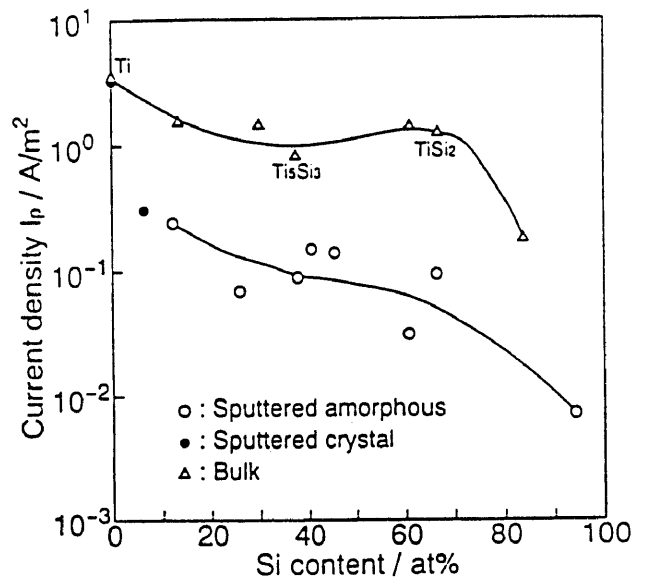Fig. 14 Anodic polarization curves of sputtered Ti-Si alloys.

Fig. 16 Compositional dependence of anodic current densities at +0.1 V(SCE) for sputtered amorphous, sputtered crystalline and crystalline bulky alloys.

In those figures the values of crystalline bulky Ti-Si alloys produced by arc-melting are also plotted. The corrosion resistance of crystalline bulky Ti-Si alloys including and TiSi$_2$ compounds is not improved by alloying Si except large amounts of Si, because the corrosion potentials of the alloys are in less noble side around 0 to -0.5 V(SCE), and the current densities of the alloys are around 10^0A/m^2. The large amounts of 80 at%Si in the crystalline Ti-Si improve the corrosion resistance of the alloys. The amorphization of Ti-Si alloys shifts the corrosion potentials to the more noble side around +0.8 V(SCE) and decreases the passive current densities of one or two order of magnitude less than the crystalline bulky Ti-Si alloys. Further, the passive current densities of Ti-Si amorphous alloys decrease with increasing Si content. These results indicate that the amorphization of Ti-Si alloys definitely improve the corrosion resistance of the alloys. The same factors in Ti-B alloys also operate in Ti-Si alloys. The amorphization of structure gives Ti-Si alloys the compositional homogeneity. Further, the amorphous Ti-Si alloys have no crystalline defects such as grain boundaries and precipitates. These factors give the alloys high corrosion resistance.

4. Conclusions

The Ti-B and Ti-Si binary alloys were prepared by argon sputtering. The structure and corrosion properties were investigated by x-ray diffraction and polarization methods.

Ti-B amorphous alloys containing B content of 8 at%B to 52 at%B were amorphous. Amorphization of Ti-B alloys shifts the corrosion potentials from -0.5 V(SCE) of

crystalline bulky Ti-B alloys to +0.3 V(SCE), and reduces the passive current densities of 10^0-10^2A/m^2 at +1.0 V(SCE) for crystalline bulky Ti-B alloys to 10^{-1} A/m^2 for Ti-B amorphous alloys.

Ti-Si amorphous alloys containing 12 at%Si or more were also prepared by sputtering. The corrosion potentials and passive current densities of Ti-Si amorphous alloys are +0.3 V(SCE) and 10^{-1}-10^{-2} A/m^2.

The amorphous Ti-B and Ti-Si alloys exhibit high corrosion resistance. The amorphization of the alloys definitely improves the corrosion resistance. The amorphization makes the alloys chemically homogeneous, and the amorphous alloys have no crystalline defects such as precipitates and crystalline boundaries. These factors clearly improve the Ti-B and Ti-Si alloys.

1) M. Naka, K. Hashimoto and T. Masumoto, J. Japan Inst. Met., **38**(1976)385.

2) M. Naka, M. Miyake, M. Maeda and I. Okamoto, Scripta Met., **17**(1983), 1293.

3) M. Naka, M. Miyake, M. Maeda and I. Okamoto, Proc. 5th Int. Conf. on Rapidly Quenched Metals, 1985, 1473.

4) M. Naka, M. Miyake and I. Okamoto, **5**(1986), 521.

5) M. Naka, K. Asami, K. hashimoto and T. masumoto, Proc. 4th Int. Conf. on Titanium, AIME, 1981, 2695.

6) M. Naka, H. Fujimori and I. Okamoto, Proc. 7th Inter. Conf. on Vacuum Metallurgy,, The Iron Steel Inst. Japan, 1982, 650.